A VLSI IMPLEMENTATION OF A NEW LOW VOLTAGE 4th ORDER DIFFERENTIAL G_m-C BAND-PASS FILTERS FOR DIFFERENT APPROXIMATION IN CMOS TECHNOLOGY

Radu Gabriel BOZOMITU Vlad CEHAN

Faculty of Electronics, Telecommunications and Information Technology, "Gh. Asachi" Technical University,
Carol I No. 11 Av., 700506, Iaşi, Romania, Phone: *+40-232-213737, bozomitu@etc.tuiasi.ro, vlcehan@etc.tuiasi.ro*

Abstract: In this paper we present a new low voltage 4th order differential G_m-C band-pass filter (BPF) for different approximations (Butterworth or Chebyshev), which has been designed in CMOS technology. This differential BPF is composed of two G_m-C biquad structures in cascade connection. The type of band-pass filter approximation (Butterworth or Chebyshev) can be set by an adequate choice of grounded capacitors, using digital command logic. The proposed G_m-C filter architecture is attractive for VLSI implementation and offers the possibility of tuning the centre frequency and the selectivity, using external biasing currents or modifying the grounded capacitor values. The proposed structure provides a ±15% corners variation of the centre frequency, a dynamic range of 200mV$_{pp(diff)}$, distortion THD<1%, and a 10mA current consumption from a 1.8V voltage supply. The simulations performed in 65nm CMOS technology confirm the theoretical results.

Key words: *G_m-C filter, biquad, transconductor, OTA, dynamic range, Butterworth, Chebyshev, CMOS, VLSI.*

I. INTRODUCTION

G_m-C filters are the most popular technique used in implementing integrated high frequency continuous-time (CT) filters [1] – [29]. Most CT filters contain integrators as basic building blocks. Their popularity stems from the fact that transconductors are very easy to implement in monolithic form, transconductors generally have higher bandwidth than operational amplifiers, they can be tuned electronically, and lead to simple circuitry [14] – [22].

The active element used to realize the voltage mode and the current mode integrators and also the active filters is the transconductor. This device influences the frequency performances of the realized filter. The *G_m-C* active filters can be implemented by using follow the leader feedback (FLF) structures having different types of transconductors (OTA with simple differential stage, CCII) built in different technologies.

One major problem occurring in active filters design is the fact that the cut-off or centre frequencies are strongly dependent of process, temperature and supply voltage variations [1] – [12]. There are many solutions to this problem reported in literature [13] – [29].

Another important problem reported in literature is represented by the narrow dynamic range of the input signal for which the circuit works linearly [23] – [29]. This issue can be solved if a higher supply voltage is used.

In this paper a new low voltage 4th order differential *G_m-C* band-pass filter (BPF) for different approximation, which solves the above constraints, has been designed in CMOS technology.

The type of BPF approximation (Butterworth or Chebyshev) can be set by an adequate choice of grounded capacitors values, using digital command logic.

The proposed structure is attractive for VLSI and offers the possibility of tuning the centre frequency and selectivity, using external biasing currents.

In Section II, the proposed filter topology is presented and analyzed by simulations at system level. Bode characteristics of the ideal 4th order differential BPF and poles distributions in complex plane are shown for both types of BPF approximations.

In Section III, the proposed low voltage 4th order differential *G_m-C* band-pass filter for both approximations (Butterworth or Chebyshev) is implemented at circuit level. The proposed transconductor cell with higher dynamic range, used in BPF implementation, is presented.

The operation of the proposed structure is illustrated in Section IV by simulations in 65nm CMOS technology.

II. THE 4th ORDER DIFFERENTIAL *G_m-C* BAND-PASS FILTER TOPOLOGY

In Fig. 1 is shown the block diagram of the proposed 4th order differential *G_m-C* band-pass filter.

The centre frequencies of the 4th order differential *G_m-C* band-pass filter from Fig. 1 can be tuned using different values of the bias currents or grounded capacitors. To obtain the centre frequencies imposed by design condition, the poles of the 4th order BPF for both, Butterworth and Chebyshev approximations, and the multiplicative constant ***K*** are presented in Table 1.

Both Bode characteristics and poles distribution of the ideal 4th order differential BPF in both types of approximations, for a centre frequency of 30MHz are illustrated in Figs. 2 and 3, respectively.

For Butterworth filters (Fig. 2), we can note that the poles lie along a circle in the s-plane [7].

The filter needs to have a frequency response as flat as mathematically possible in the pass-band, that is, it should be a *maximally flat magnitude filter*.

Manuscript received July 30, 2009; revised October 14, 2009

Chebyshev filters (Fig. 3) are analog or digital filters with a steeper roll-off and more pass-band ripple (type I) or stop-band ripple (type II) than Butterworth filters. The former minimize the error between the idealized filter characteristic and the actual over the range of the filter, but with ripples in the pass-band [7].

Due to the pass-band ripple inherent in Chebyshev filters, the filters which have a smoother response in the pass-band, but a more irregular response in the stop-band are preferred for some applications. For Chebyshev filters poles are arranged on an ellipse in the s-plane [7].

From Fig. 1, the transfer function of the 4th order differential G_m-C band-pass filter in different approximations can be written:

$$H(s) = \frac{(G_{m1}/C_1)s}{s^2 + s\frac{G_m}{C_1} + \frac{G_m^2}{C_1C_2}} \cdot \frac{(G_{m2}/C_3)s}{s^2 + s\frac{G_m}{C_3} + \frac{G_m^2}{C_3C_4}} \quad (1)$$

where

$$K = \frac{G_{m1}}{C_1} \cdot \frac{G_{m2}}{C_3} \quad (2)$$

is the multiplicative constant presented in Table 1.

Table 1. Poles of the 4th order BPF in Butterworth and Chebyshev approximations depend on centre frequency

Filter type	Butterworth	Chebyshev
Centre frequency [MHz]	30	30
Gain at centre frequency	1	1
LF poles x 10^6 [Hz]	-6.244 ±j·21.273	-4.414 ±j·20.18
HF poles x 10^6 [Hz]	-11.433 ±j·38.95	-9.308 ±j·42.56
K	2.4674e+016	2.4245e+016

From the poles distribution in complex plane illustrated in Figs. 2 and 3, for both approximations, the poles of the 4th order differential G_m-C band-pass filter, having the transfer function presented in equation (1), can be noted as follows:

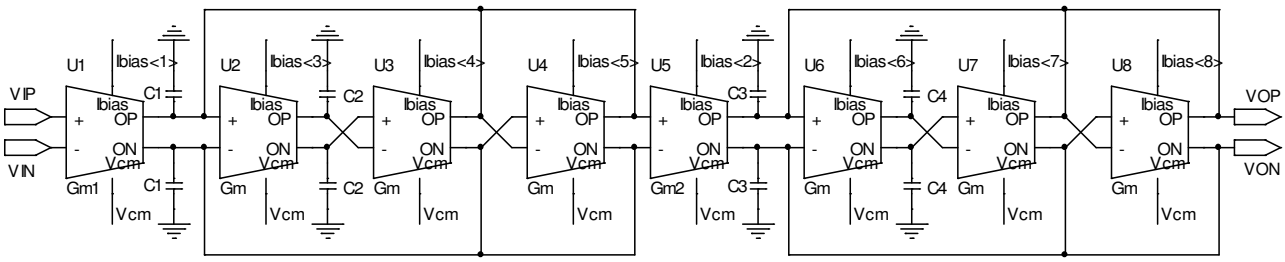

Figure 1. Block diagram of 4th order differential G_m-C band-pass filter

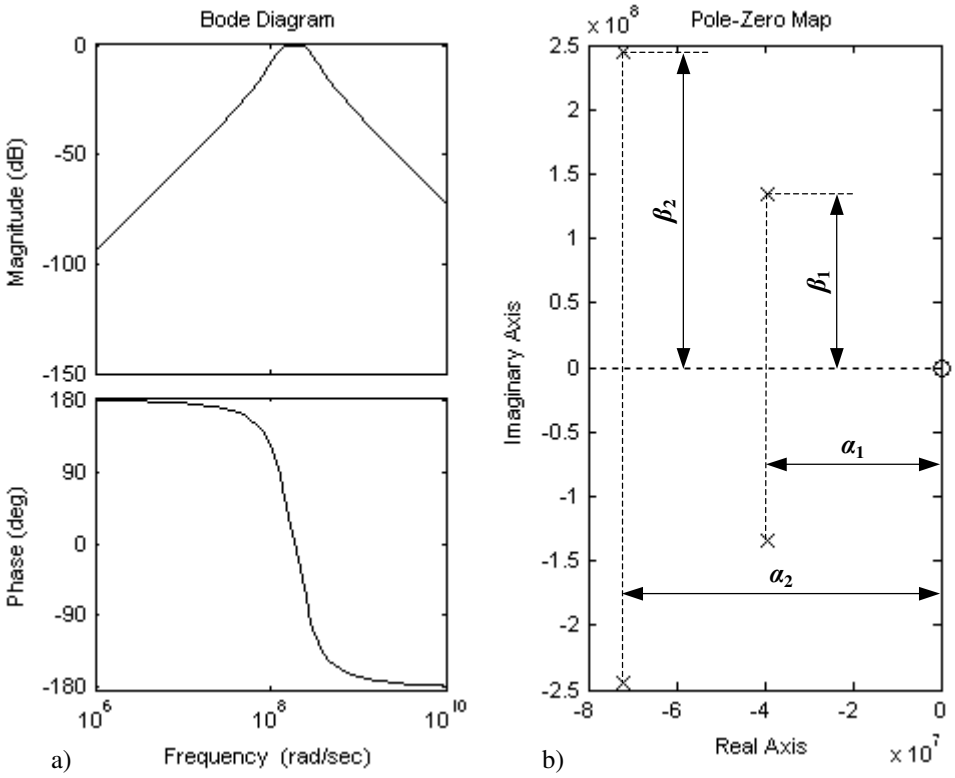

Figure 2. Bode characteristics of the ideal 4th order differential Butterworth type BPF (a) and poles distribution (b) for a centre frequency of 30 MHz

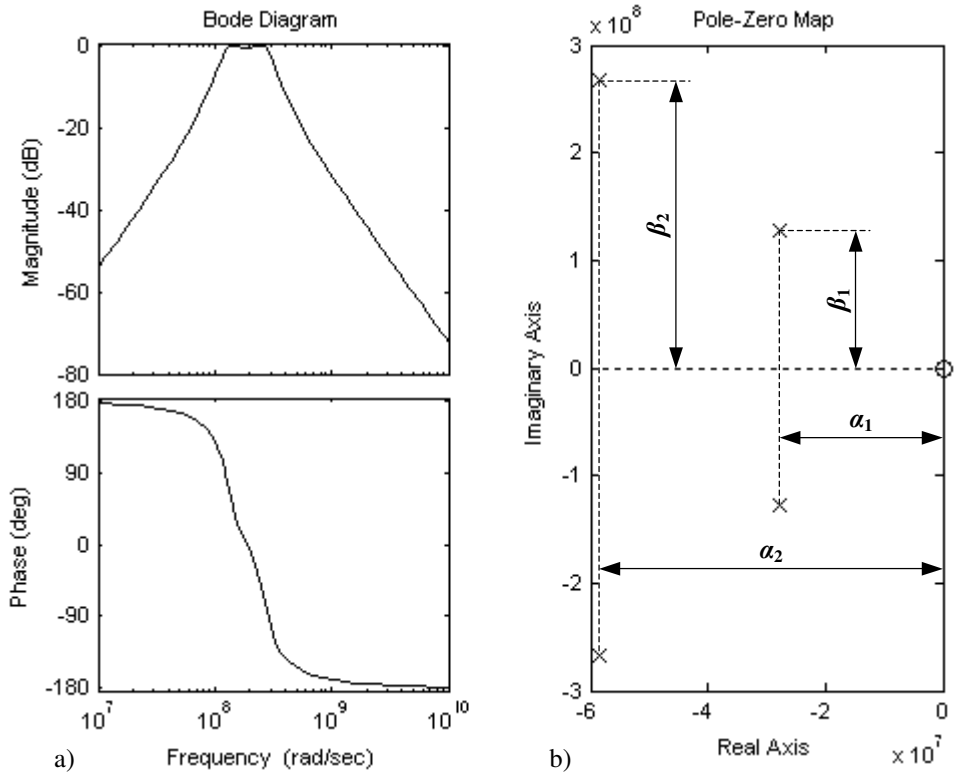

Figure 3. Bode characteristics of the ideal 4th order differential Chebyshev type BPF (a) and poles distribution (b) for a centre frequency of 30 MHz

$$\begin{cases} p_{1,2} = \alpha_1 \pm j\beta_1 \\ p_{3,4} = \alpha_2 \pm j\beta_2 \end{cases} \quad (3)$$

Using the poles expressions in (3) in the denominator of the BPF transfer function from equation (1), by terms identification, one can obtain the grounded capacitor values:

$$\begin{cases} C_1 = -\dfrac{G_m}{2\alpha_1} \\ C_2 = -\dfrac{2\alpha_1 \cdot G_m}{\alpha_1^2 + \beta_1^2} \\ C_3 = -\dfrac{G_m}{2\alpha_2} \\ C_4 = -\dfrac{2\alpha_2 \cdot G_m}{\alpha_2^2 + \beta_2^2} \end{cases} \quad (4)$$

It is important to note that for the multiplicative constant K presented in Table 1, the proposed 4th order differential G_m-C band-pass filter in both approximations has unitary voltage gain at centre frequency.

Knowing the multiplicative constant K, from equation (2) one can determine the G_{m1} and G_{m2} transconductances values (illustrated in Fig. 1) so that the proposed BPF had unitary voltage gain at centre frequency.

Knowing the poles values of the 4th order differential G_m-C BPF in both approximations (Butterworth and Chebyshev) given by (α_1, β_1), (α_2, β_2) in equations (3) and Figs. 2 and 3, and choosing an appropriate value for differential transconductance G_m in Fig. 1 (i.e. G_m = **1mS**), the values of the grounded capacitors dependent on centre frequencies are presented in Table 2. The capacitors used (nMOS in nwell process) are provided by the technology. They are implemented on the base of nMOS transistors, having the capacitance value dependent on the aspect ratio (W/L) of the transistor.

Table 2. Grounded capacitors depending on centre frequencies of the 4th order differential G_m-C band-pass filter in Butterworth and Chebyshev approximations

C / Type/Freq	C_1 [pF]	C_2 [pF]	C_3 [pF]	C_4 [pF]
Butterworth 30MHz	12.7	4	7	2.2
Chebyshev 30MHz	18	3.3	8.5	1.6

The G_m transconductor shown in the block diagram in Fig. 1 can be implemented using a differential operational transconductance amplifier (OTA) designed for an extended dynamic range linear operation.

The bandwidth of the proposed 4th order differential G_m-C BPF in both approximations is between (20 – 45)MHz as design conditions. For Chebyshev type BPF a band-pass ripple of 1dB has been considered. Thus, the centre frequency of BPF in both approximations is 30MHz.

III. IMPLEMENTATION OF THE G_m TRANSCONDUCTOR CELL AT THE TRANSISTOR LEVEL

In Fig. 4 is presented the electric scheme of the G_m transconductor.

The proposed G_m transconductor in Fig. 4 is formed of a differential pair implemented with M_1 and M_2 transistors and a common mode feedback (CMFB) loop represented by M_3 – M_6 transistors. The linearity of the proposed transconductor can be sensitively improved by using a topology with M_9 and M_{10} transistors [2].

For the transconductor illustrated in Fig. 4, the classic resistive degeneration has been replaced by MOSFET transistors M_9 and M_{10} operating in deep triode region.

For this structure, M_9 and M_{10} are in deep triode region if $V_{in} = 0$. As the gate voltage of M_1 becomes more positive than the gate voltage of M_2, transistor M_9 stays in the triode region with $V_{D9} = V_{G9} - V_{GS1}$ whereas M_{10} eventually enters the saturation region because its drain voltage rises and its gate and source voltage fall.

Thus, the circuit remains relatively linear even if one degeneration device goes into saturation.

For the widest linear region [9] suggests:

$$\left(\frac{W}{L}\right)_{1,2} \approx 7\left(\frac{W}{L}\right)_{9,10} \tag{5}$$

Since the proposed transconductor in Fig. 4 provides a higher dynamic range by using a linearity technique implemented with M_9 and M_{10} transistors, a trade-off between linearity and tunability has to be consider in this transconductor cell design. Using this linearity technique, a linear transconductor will be obtained, but the transconductance value G_m will provide very little dependence on the bias currents. Thus the centre frequencies of the proposed BPF in both approximations can be tuned better by modifying the grounded capacitors values.

IV. SIMULATION RESULTS

The operation of the proposed 4th order differential G_m-C band-pass filter in both, Butterworth and Chebyshev approximations are analyzed by simulations in 65nm CMOS technology.

An input signal of $200mV_{pp(diff)}$ and 1.8V supply voltage is used.

First, the operation of the proposed transconductor cell (G_m-cell) in Fig. 4 is analyzed.

In both Figs. 5 and 6 are shown differential output currents and voltages dependence on the input voltage of the G_m-cell, for a unitary voltage gain and for $I_{bias} = 80\mu A$.

In Fig. 7 is presented the differential transconductance dependence on input voltage for a unitary voltage gain and for $I_{bias} = 80\mu A$. From this dc simulation a value of the differential transconuctance $G_m = 1mS$ is obtained and the dynamic range of the input signal for which the circuit transconductor operates linearly is about $400mV_{pp(diff)}$. The dynamic range represents the range values of the input signal for which the transconductance value is constant and independent of the input voltage with an error $\varepsilon \le 1\%$.

In Fig. 8 is presented the differential voltage gain dependence on the input voltage of the G_m-cell for I_{bias}=80µA.

In Fig. 9 is shown the AC frequency response of the G_m-cell in closed loop operation (unitary voltage gain) for I_{bias}=80µA.

In Fig. 10, the AC frequency response of the G_m-cell in open loop for I_{bias}=80µA is presented. The gain of the proposed transconductor is of about 32dB.

The maximum frequency operation of the proposed structure depends on G_m/C ratio. In order to obtain high frequency, this ratio must be as high as possible. The transconductance value G_m is limited by the trade-off between gain and linearity (i.e. a high transconductance value implies narrow dynamic range). The frequency operation range can also be increased by minimizing the grounded capacitors values, but these can be minimized only

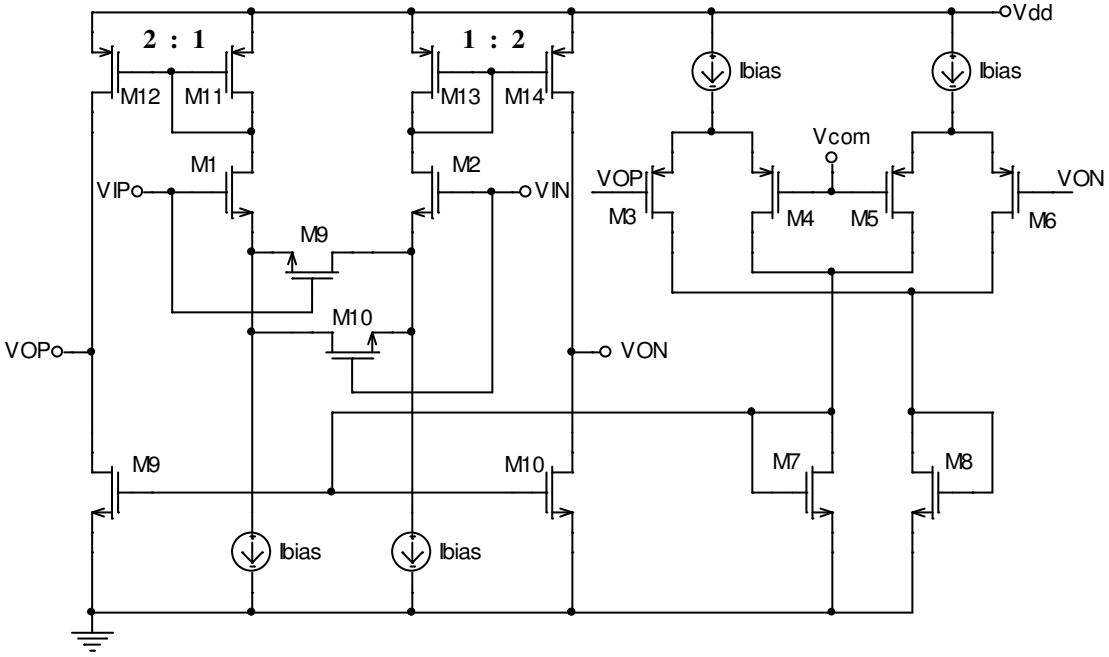

Figure 4. Electric scheme of the transconductor from G_m-C filter

up to parasitic capacitors values.

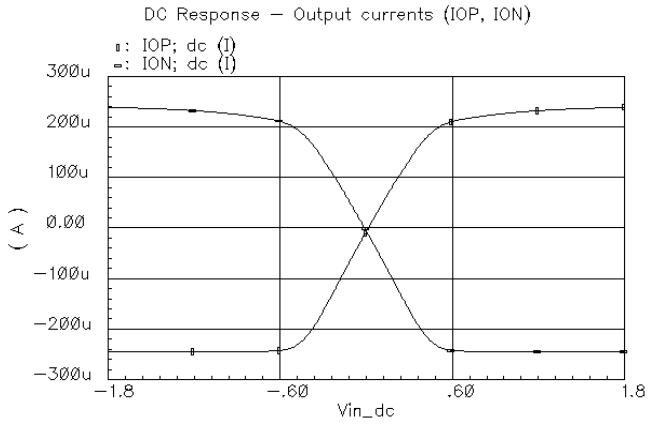

Figure 5. Differential output currents of the G_m-cell for a unitary voltage gain (I_{bias}=80μA)

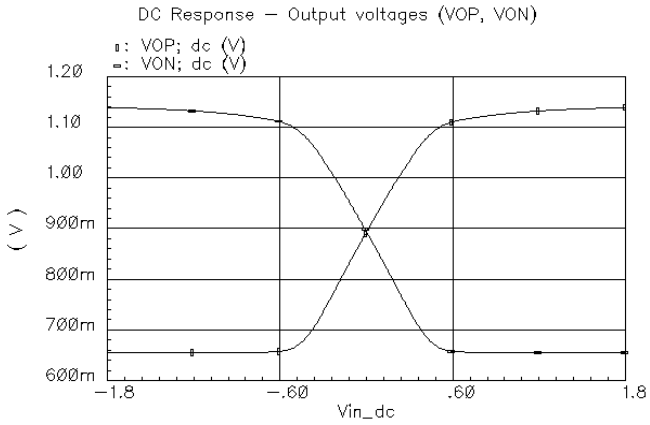

Figure 6. Differential output voltages of the G_m-cell for a unitary voltage gain (I_{bias}=80μA)

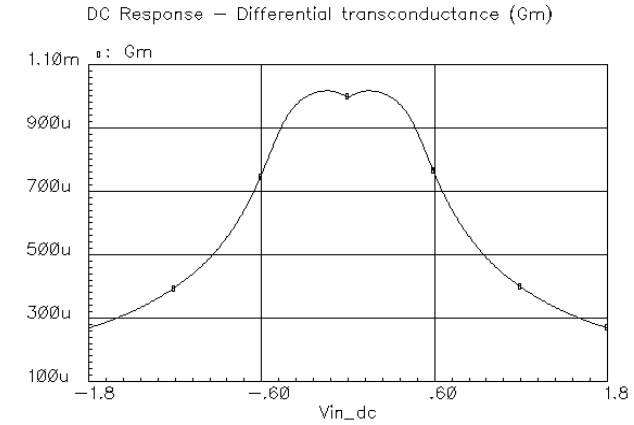

Figure 7. Differential transconductance for a unitary voltage gain (I_{bias}=80μA)

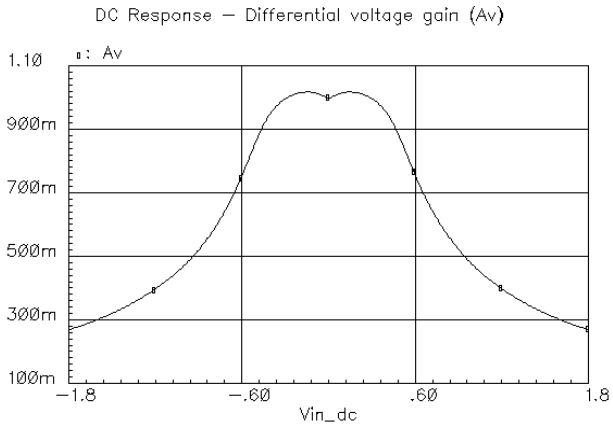

Figure 8. Differential voltage gain of G_m-cell (I_{bias}=80μA)

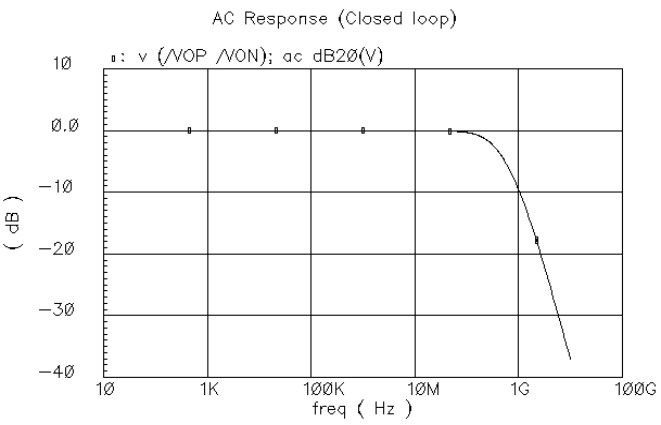

Figure 9. AC frequency response of G_m-cell in closed loop (unitary voltage gain) (I_{bias}=80μA)

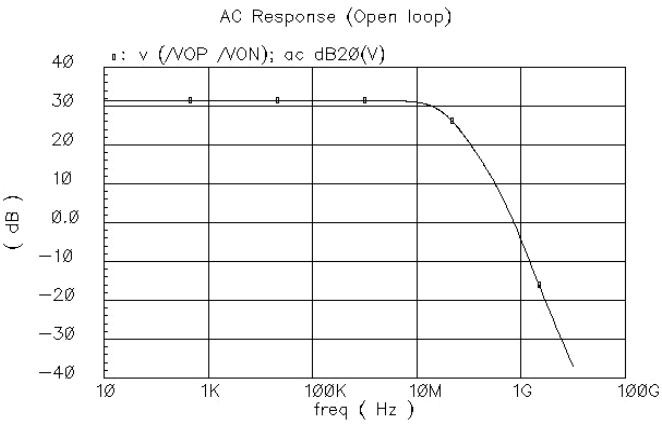

Figure 10. AC frequency response of G_m-cell in open loop (I_{bias}=80μA, R_{load} = 1MΩ)

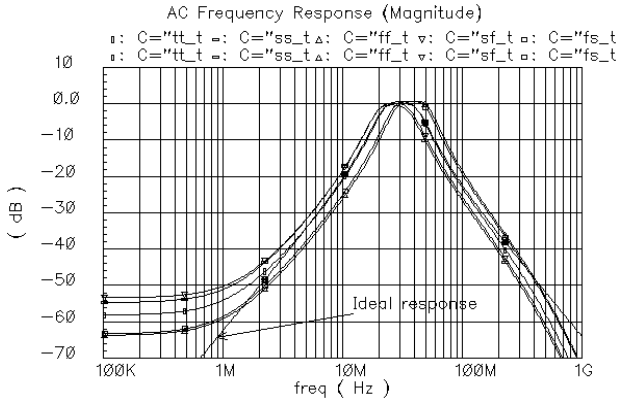

Figure 11. AC frequency response (magnitude) of the proposed BPF in Butterworth approximation depending on corners

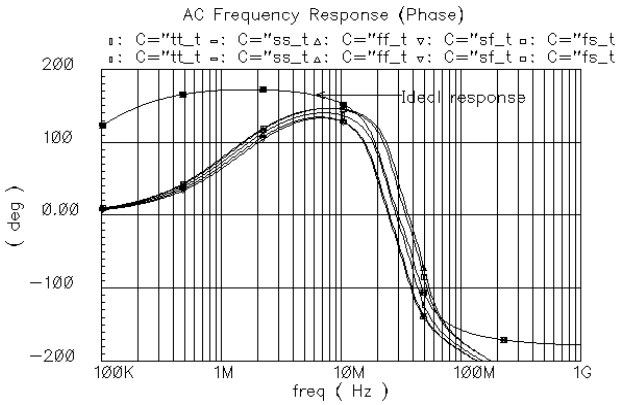

Figure 12. AC frequency response (phase) of the proposed BPF in Butterworth approximation depending on corners

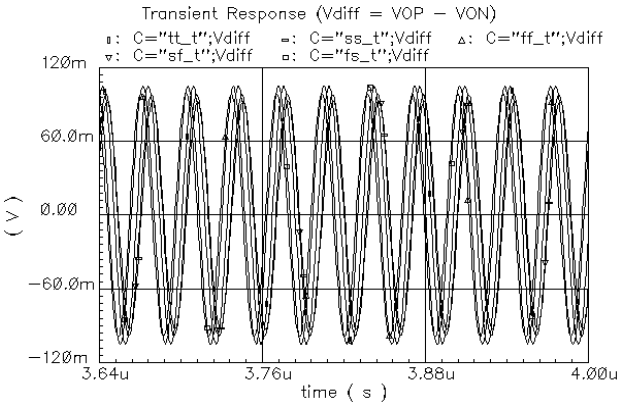

Figure 13. Differential output voltages of the proposed BPF in Butterworth approximation depending on corners

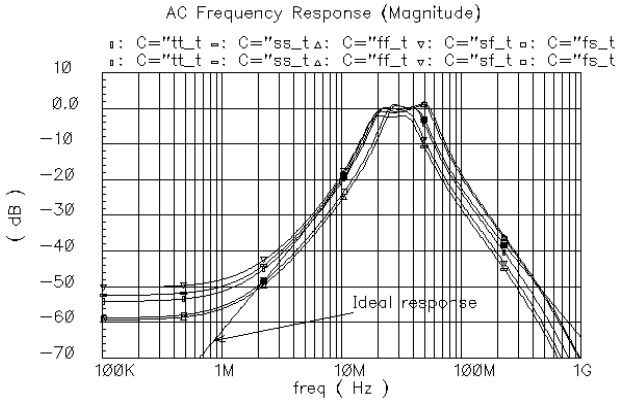

Figure 14. AC frequency response (magnitude) of the proposed BPF in Chebyshev approximation depending on corners

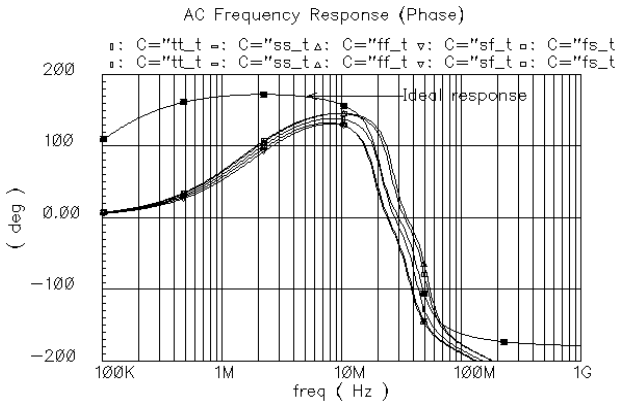

Figure 15. AC frequency response (phase) of the proposed BPF in Chebyshev approximation depending on corners

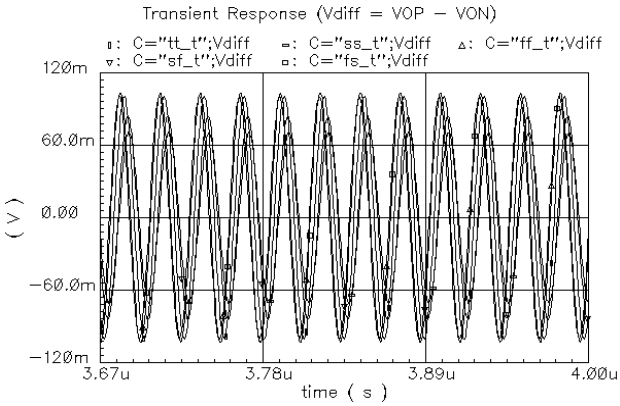

Figure 16. Differential output voltages of the proposed BPF in Chebyshev approximation depending on corners

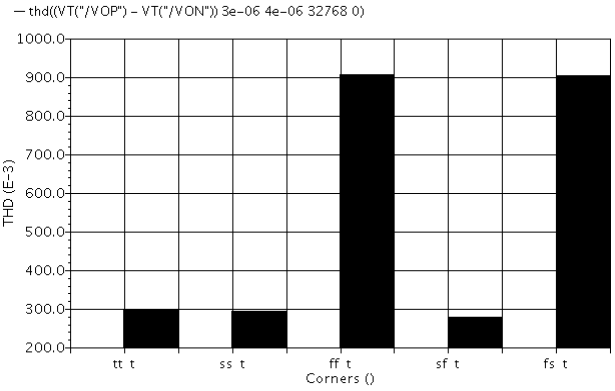

Figure 17. THD of the differential output voltage of the proposed BPF in Butterworth approximation depending on corners

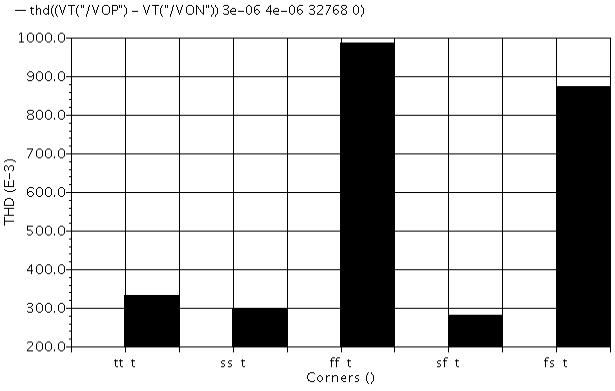

Figure 18. THD of the differential output voltage of the proposed BPF in Chebyshev approximation depending on corners

Taking into consideration the above observation, the maximum frequency operation of the proposed structure is of about 50 MHz.

Next, the AC simulations of the 4th order differential G_m-C band-pass filter for Fig. 1 in both Butterworth and Chebyshev approximations are made in different critical corners, using the grounded capacitor values illustrated in Table 2.

In order to verify the correct operation of the proposed BPF, the following simulations have been made in five critical corners, illustrated in Table 3.

Table 3. Corners considered in BPF simulations

Process	Temperature	Supply voltage
Typical (tt_t)	75°	PS=1.8V
Slow (ss_t)	125°	PS=1.62V
Fast (ff_t)	0°	PS=1.98V
Slow-fast (sf_t)	125°	PS=1.62V
Fast-slow (fs_t)	0°	PS=1.98V

In Figs. 11 and 12 are presented the small signal frequency responses (magnitude and phase versus frequency) of the proposed 4th order differential G_m-C Butterworth type band-pass filter (in Fig. 1) for a centre frequency of 30MHz given by AC simulations performed in all critical corners (Table 3).

In order to obtain a unitary voltage gain at centre frequency, the transconductor cells $\boldsymbol{G_{m1}}$ and $\boldsymbol{G_{m2}}$ in Fig. 1 have been biased with $\boldsymbol{I_{bias1}}$ **= 130µA**, so that the equation (2) be fulfilled in Butterworth approximation. For all other transconductor cells a $\boldsymbol{I_{bias}}$ **= 80µA** has been used.

In order to validate the Butterworth type characteristics, the Bode characteristics (magnitude and phase) provided by the proposed BPF (shown in Figs. 11 and 12) are overlapped with the ideal Bode characteristics given by the ideal 4th order differential G_m-C Butterworth type band-pass filter, implemented at system level. From Figs. 11 and 12 we can see that both Bode characteristics (real and ideal) are very close in interest frequency range.

In Fig. 13 are presented the differential output voltages of the proposed BPF in Butterworth approximation depending on corners; a very small variation of these waveforms has been obtained.

In Figs. 14 and 15 are presented the small signal frequency responses (magnitude and phase versus frequency) of the proposed 4th order differential G_m-C Chebyshev type band-pass filter in Fig. 1, for centre frequencies of 30MHz, given by AC simulations performed in all critical corners (Table 3).

In order to obtain a unitary voltage gain at centre frequency, the transconductor cells $\boldsymbol{G_{m1}}$ and $\boldsymbol{G_{m2}}$ in Fig. 1 have been biased with $\boldsymbol{I_{bias1}}$ **= 200µA**, so that the equation (2) be fulfilled in Chebyshev approximation. For all other transconductor cells a $\boldsymbol{I_{bias}}$ **= 80µA** has been used.

In order to validate the Chebyshev type characteristics, the Bode characteristics (magnitude and phase) provided by the proposed BPF (shown in Figs. 14 and 15) are overlapped with the ideal Bode characteristics given by the ideal 4th order differential G_m-C Chebyshev type band-pass filter, implemented at system level. From Figs. 14 and 15 we can see that both real and ideal Bode characteristics are very close in interest frequency range.

In Fig. 16 are presented the differential output voltages of the proposed BPF in Chebyshev approximation depending on corners; a very small variation of these waveforms has been obtained.

In Figs. 17 and 18 are presented the THD values of the differential output signal of the proposed 4th order differential G_m-C band-pass filter in both approximations (Butterworth and Chebyshev), for a 30MHz centre frequency, obtained by transient simulations performed in all critical corners. From these simulations a $\boldsymbol{THD \leq 1\%}$ has been obtained in both approximations for all corners and centre frequencies imposed by design conditions.

According to these simulation results, the 4th order differential G_m-C band-pass filter in both approximations (Butterworth and Chebyshev) provides a ±15% corners variation of the centre frequency.

V. CONCLUSIONS

In this paper a new low voltage 4th order differential G_m-C band-pass filter in Butterworth and Chebyshev approximations has been presented.

The type of band-pass filter approximation (Butterworth or Chebyshev) can be set by an adequate choice of grounded capacitors, using digital command logic.

The centre frequency and selectivity of the proposed band-pass filter in both approximations can be modified by using different values of grounded capacitors or external bias currents.

The frequency performances of the proposed band-pass filter depends on the $\boldsymbol{G_m/C}$ ratio. In order to increase the frequency operation, on one hand the transconductance $\boldsymbol{G_m}$ of the transconductor cell has to be as high as possible, and on the other hand, the grounded capacitors have to be minimized up to parasitic values.

The proposed structure provides a ±15% corners variation of the centre frequency, a dynamic range of $200mV_{pp(diff)}$, distortion THD<1%, and a 10mA current consumption from a 1.8V supply voltage.

The simulations performed in a 65nm CMOS technology confirm the theoretic results.

REFERENCES

[1] David Johns, Ken Martin, *„Analog Integrated Circuit Design”*, John Wiley & Sons, Inc., 1997;

[2] Behzad Razavi, “Design of Analog CMOS Integrated Circuits”, McGraw-Hill Higher Education, Inc., 2001;

[3] Kenneth R. Laker, Willy M. C. Sansen, *„Design of Analog Integrated Circuits and Systems”*, McGraw-Hill, New York, 1994;

[4] C. Toumazou, F. J. Lidgey, and D. G. Haigh (eds.), *„Analogue IC Design: The Current-Mode Approach”*, London: Peter Peregrinus Ltd., 1990;

[5] Paul R. Gray, Robert G. Meyer, *„Circuite Integrate Analogice - Analiză şi Proiectare”*, Edit. Tehnică, Bucureşti, 1999;

[6] L. P. Huelsman and P. E. Allen, *„Introduction to the Theory and Design of Active Filters”*, New York: McGraw-Hill Inc., 1980;

[7] Adel S. Sedra and Peter O. Brackett, *„Filter Theory and Design: Active and Passive”*, Pitman Publishing Limited, London, 1978;

[8] R. Schaumann, S. M. Ghausi and K. R. Laker, *„Design of Analog Filters: Passive, Active RC and Switched Capacitor”*, Pretince-Hall, Englewood Cliffs, NJ, 1990;

[9] F. Krummenacher and N. Joehl, “A 4-MHz CMOS Continous-Time Filter with On-Chip Automatic Tuning”, *IEEE J. Solid-State Circuits*, vol. 23, pp. 750-758, June 1988;

[10] Chun-Ming Chang, „New Multifunction OTA-C Biquads”, *IEEE Trans. on Circuits and Systems – II*, vol. 46, no. 6, pp. 820-823, June 1999;

[11] Chun-Ming Chang and Shih-Kuang Pai, „Universal Current-Mode OTA-C Biquad with the Minimum Components”, *IEEE Trans. on Circuits and Systems – I*, vol. 47, no. 8, pp. 1235-1238, August 2000;

[12] Hanspeter Schmid, „Approximating the Universal Active Element”, *IEEE Transactions on Circuits and Systems - II: Analog and Digital Signal Processing*, vol. 47, no. 11, pp. 1160-1169, November 2000;

[13] Jirayuth Mahattanakul and Chris Toumazou, „Current-Mode Versus Voltage-Mode G_m-C Biquad Filters: What the Theory Says”, *IEEE Transactions on Circuits and Systems – II: Analog and Digital Signal Processing*, vol. 45, no. 2, pp. 173-186, February 1998.

[14] Rainer Nawrocki, „Electronically Controlled OTA-C Filter with Follow-the-Leader-Feedback Structure”, *International Journal of Circuit Theory and Applications*, vol. 16, pp. 93-96, 1998;

[15] Y. P. Tsividis, „Integrated continuous-time filter design – An overview”, *IEEE J. Solid-State Circuits*, vol. 29, pp. 166-176, Mar. 1994;

[16] Randall L. Geiger and Edgar Sanchez-Sinencio, „Active Filter Design Using Operational Transconductance Amplifiers: A tutorial”, *IEEE Circuits and Devices Magazine*, vol. 1, pp. 20-32, 1985;

[17] E. Sanchez-Sinencio, R. L. Geiger and H. Nevarez-Lozano, „Generation of continuous-time two integrator loop OTA filter structures”, *IEEE Trans. Circuits and Systems*, CAS-35, pp. 936-946, 1988;

[18] H. Nevarez-Lozano, A. Hill and E. Sanchez-Sinencio, „Frequency limitations of continuous-time OTA-C filters”, *Proc. IEEE Int. Symp. on Circuits and Systems*, Espoo, IEEE, vol. 3, pp. 2169-2172, 1988;

[19] C. Acar, F. Anday and H. Kuntman, „On the Realization of OTA-C Filters”, *International Journal of Circuit Theory and Applications*, vol. 21, pp. 331-341, 1993;

[20] Henrique S. Malvar, „Electronically Tunable Active Filters with Operational Transconductance Amplifiers”, *IEEE Trans. on Circuits and Systems*, vol. CAS-29, no. 5, pp. 333-336, May 1982;

[21] Tim Bakken and John Choma Jr., „Stability of a Continuous-Time State Variable filter with OPAMP and OTA-C Integrators”, *Great Lakes Symposium on VLSI*, February 1998;

[22] Tim Bakken and John Choma Jr., „Stability of a Continuous-Time State Variable filter with ORA-L and Current Amplifiers Integrators”, *Great Lakes Symposium on VLSI*, February 1998;

[23] Wu P., R. Schaumann and S. Szczepanski, „A CMOS OTA with Improved Linearity Based on Current Addition”, *Proc. IEEE Int. Symp. Circuits Syst.*, 1990;

[24] Gert Groenewold, „The Design of High Dynamic Range Continuous-Time Integratable Bandpass Filters”, *IEEE Trans. on Circuits and Systems*, vol. 38, no. 8, pp. 838-852, August 1991;

[25] Nabil I. Khachab, Abdulaziz Al-Saquer and Joji G. Varghese, „A BiCMOS Cell with Applications to Highly Linear Analog Transconductor Realizations”, *IEEE Transactions*, 1996;

[26] Peter Bowron, K. A. Mezher and A. A. Muhieddine, „The Dynamic Range of Second-Order Continuous-Time Active Filters”, *IEEE Trans. on Circuits and Systems – I*, vol. 43, no. 5, pp. 370-373, May 1996;

[27] Y. Tsividis, M. Banu and J. Khoury, „Continuous-time MOSFET-C filters in VLSI”, *IEEE J. Solid-State Circuits*, vol. SC-21, pp. 15-30, Feb. 1986;

[28] Y. Tsividis and J. O. Voorman, Eds., *Integrated Continuous-Time Filters*, Piscataway: IEEE Press, 1993;

[29] Edgar Sánchez-Sinencio, Jaime Ramirez-Angulo, Bernabé Linares-Barranco and Angel Rodriguez-Vázquez, „Operational Transconductance Amplifier-Based Nonlinear Function Syntheses”, *IEEE Journal of Solid-State Circuits*, vol. 24, no. 6, pp. 1576-1586, December 1989.